Laser-assisted formation of antihydrogen

R. J. Whitehead*
Department of Physics, University of Durham, Durham DH1 3LE, United Kingdom

J. F. McCann
Department of Applied Mathematics and Theoretical Physics, Queen's University, Belfast BT7 1NN, United Kingdom

I. Shimamura
Institute of Physical and Chemical Research (RIKEN), Hirosawa, Wako-shi, Saitama 351-0198, Japan
(Received 21 June 2000; published 26 June 2001)

Capture of slow antiprotons by atomic hydrogen and positronium is simulated by the classical trajectory Monte Carlo method. Statistically accurate cross sections for protonium and antihydrogen formation are obtained and the energy dependence of the process is established. The results agree very well with experimental data for proton capture by positronium. Antihydrogen formation from antiproton-positronium collisions in the presence of a laser is simulated and the effects of laser polarization, frequency, and intensity are studied. Enhancements of the antihydrogen formation cross section are observed. For example, an increase of 70% is found for light of intensity 1.4×10^{13} W cm^{-2} and wavelength $\lambda=248$ nm, for an antiproton collision energy of 1 keV.

DOI: 10.1103/PhysRevA.64.0134XX PACS number(s): 34.50.Rk, 36.10.Dr

I. INTRODUCTION

The interaction of antiprotons with simple atoms has been a subject of great importance since the development of low-energy antiproton beams. Two issues of current interest relate to the capture of antiprotons by atoms, namely the spectroscopy of cold antihydrogen [1] and the dynamics of highly excited antiprotonic atoms [2–4]. At the core of these studies is the knowledge of the rate of formation of these systems and the nature of the states that are formed. Our paper presents the results of classical simulations for processes leading to the formation of such systems. In particular, we calculate cross sections for antiproton capture by atomic hydrogen to form protonium, and by positronium to form antihydrogen. We investigate the effects of the presence of a laser on the antihydrogen formation rate.

The predominant inelastic process arising from fast antiproton collisions with atoms or molecules is ionization of the target. Antiproton ionizing collisions are well understood at present, except perhaps at collision energies far below the ionization threshold, and the topic has been comprehensively discussed by Knudsen and Reading [5]. According to theory, below the ionization threshold, the importance of capture increases rapidly. An overview of theoretical approaches to antiproton capture by small atoms and molecules has been given recently by Cohen [6,7], in which the role of classical modeling was highlighted. The classical trajectory Monte Carlo (CTMC) method was introduced by Abrines and Percival [8] to calculate capture and ionization cross sections for proton-hydrogen collisions. It has been applied extensively in ion-atom collision studies to predict excitation and rearrangement processes in three-body processes [9]. It has been particularly successful in quantitative estimates of electron-capture cross sections over a broad region of energies around the collisional ionization threshold. The main advantage of the CTMC method is that it is relatively simple and inexpensive to execute for three-body systems without approximation. Converged fully quantum-mechanical or semiclassical simulations often require very large-scale computation. Extensions of the classical theory to cover antiproton capture by multielectron atomic and molecular targets [10] have been applied with some success [6,11]. Indeed, in the case of μ^--H collisions, the classical method performs remarkably well for muon capture below the ionization threshold when compared with methods that treat the electron quantally [12,13]. It is well suited to atomic collisions involving muons, antiprotons, and pions as it offers a fully consistent treatment of the collision process and treats all possible reaction channels on an equal footing.

In this paper, we consider the following processes:

$$\bar{p}+(T,e^-)\rightarrow\begin{cases}\bar{p}+(T,e^-)_{n,l} & \text{elastic/inelastic scattering}\\ (T,\bar{p})_{n,l}+e^- & \text{antiproton capture}\\ \bar{p}+T+e^- & \text{ionization,}\end{cases}\tag{1.1}$$

in which the target ''nucleus'' (T) can be either a proton or positron, and the reaction can take place in the presence of external fields.

II. THEORY

Consider the three-body problem in which the ith particle mass and coordinate are labeled as m_i and $\boldsymbol{r}_i$, respectively. The two-body combined mass is denoted by $m_{ij}\equiv m_i+m_j$ and the interparticle distance by $\boldsymbol{r}_{ij}=\boldsymbol{r}_j-\boldsymbol{r}_i$. Then the Jacobi coordinates can be written as $\boldsymbol{R}_{ij,k}=\boldsymbol{r}_k-\boldsymbol{R}_{ij}=\boldsymbol{r}_k-(m_i\boldsymbol{r}_i$

*Electronic address: Richard.Whitehead@physics.org

$+m_j\boldsymbol{r}_j)/m_{ij}$. The Hamiltonian in the center-of-mass frame is given by

$$H=\frac{p_{12}^2}{2\mu_{12}}+\frac{p_{12,3}^2}{2\mu_{12,3}}+\sum_{i<j}\frac{k_{ij}}{r_{ij}}, \tag{2.1}$$

where

$$\mu_{ij}=m_i m_j m_{ij}^{-1}, \tag{2.2a}$$

$$\mu_{ij,k}=m_{ij}m_k M^{-1} \tag{2.2b}$$

are reduced masses, and $M=m_{12}+m_3$ is the total mass. The momenta are defined as $\boldsymbol{p}_{ij}\equiv\mu_{ij}\dot{\boldsymbol{r}}_{ij}$ and $\boldsymbol{p}_{ij,k}\equiv\mu_{ij,k}\dot{\boldsymbol{R}}_{ij,k}$. In atomic units, $k_{ij}=Z_iZ_j$, where Z_i is the charge of the ith particle. In our case, $Z_1Z_2<0$ and $Z_2Z_3<0$, so that the projectile (particle 3) can bind with particle 2.

The CTMC procedure is well documented [8,7,14], but briefly it consists of the following steps: (i) Monte Carlo sampling of initial conditions ($t=0$), (ii) integration of the equations of motion, and (iii) identification of the exit channel in the asymptotic region $t\rightarrow+\infty$. For a given collision energy (E), the initial conditions are specified by six parameters: five for the target and one for the projectile. The projectile is launched towards the target from a prescribed fixed distance (d) with a variable impact parameter (b). The center-of-mass collision energy, E, is related to the laboratory collision energy, $E_{\rm lab}$, by

$$E=E_{\rm lab}m_{12}/M \tag{2.3}$$

and to the relative velocity of collision by

$$v=\sqrt{2E/\mu_{12,3}}. \tag{2.4}$$

The target state is modeled by the microcanonical distribution [8,14], which prescribes the sampling of momentum and position phase space subject to the constraint of fixed energy. The five free variables include three angles, two describing the orientation of the orbital plane with the third specifying the orientation of the axis of the elliptical orbit. Finally, the angular momentum and initial position of the target particles on the orbital path are chosen randomly. Implicitly, we assume that the perturbing ion is sufficiently distant, and/or the laser pulse has not yet arrived, such that the two-body motion is purely Keplerian.

The collision dynamics can be solved by integration of the equations of motion in either the Hamiltonian or Lagrangian form. The Hamiltonian formalism has been favored in the past as it is more efficient in the use of symmetry arguments that reduce the computation. In practice, it is simple and effective to work with the physically equivalent six (independent) second-order differential equations of motion following directly from Newton's second law. These were solved by resolving the equations into their Cartesian coordinates resulting in 12 first-order coupled ordinary differential equations, and integrated by an eighth-order Runge-Kutta method [15].

At intervals, a series of tests are performed in order to determine if the collision is over, and if so, the exit channel is identified. These tests are similar to those of [14]. For antiproton capture, one can associate semiquantal numbers to label the captured state according to its energy and angular momentum [9,14]. The semiquantal integers (n,l) are connected to the classical, continuous numbers n_c,l_c by the relations

$$[(n-1)(n-\tfrac{1}{2})n]^{1/3}\leqslant n_c\leqslant[n(n+\tfrac{1}{2})(n+1)]^{1/3}, \tag{2.5}$$

$$l<(n/n_c)l_c\leqslant l+1, \tag{2.6}$$

where $n_c=(\mu_{23}/2|E_{23}|)^{1/2}$, E_{23} is the energy of the bound state in its center-of-mass frame, and $l_c=|\boldsymbol{r}_{23}\times\boldsymbol{p}_{23}|$.

The presence of a laser introduces a perturbation that, in the dipole approximation and with the choice of the length gauge, has the form

$$H'=-F(t)\cos(\omega t+\varphi)\sum Z_i\boldsymbol{r}_i\cdot\boldsymbol{e}, \tag{2.7}$$

where $\boldsymbol{e}$ is the direction of polarization of the laser, ω is the angular frequency, and $F(t)$ is the electric-field amplitude. The phase of the laser φ is significant whenever the optical cycle time is longer than the time taken for the collision interaction. At higher velocities, it is necessary to choose a random selection of phases to allow for this variability. The peak field ($F_{\rm max}$) is related to the light intensity (I) by $F_{\rm max}=\sqrt{2I/\varepsilon_0 c}$. We note that the presence of the laser leads to a very small oscillatory motion of the center of mass of the system. However, this oscillatory motion dies away with the passage of the light pulse, and in the dipole approximation does not create a net transfer of momentum. In our scheme, the positronium is formed prior to the arrival of the laser pulse, and the collision products are observed after the pulse has ended. Thus the two-body bound-state quantum numbers and momentum-position distributions can be treated as field-free motions. The field was ramped smoothly on and off over a time scale τ:

$$F(t)=F_{\rm max}\begin{cases}\sin^2(\pi t/2\tau), & 0\leqslant t\leqslant\tau\\ 1, & \tau<t<\Delta T-\tau\\ \sin^2(\pi(\Delta T-t)/2\tau), & \Delta T-\tau\leqslant t\leqslant\Delta T.\end{cases} \tag{2.8}$$

A large number (N) of collisions are simulated that sample the full range of particle phase space and take into account the random laser phase. The cross sections for capture (σ^c) and ionization (σ^i) are calculated by quadrature:

$$\sigma^{c,i}=2\pi\sum_{j,k}p^{c,i}(j,b_j)b_j w_k\Delta b_k, \tag{2.9}$$

where $p^{c,i}(j,b_j)$ is the probability of a capture/ionization event happening at an impact parameter $b_k\leqslant b_j\leqslant b_k+\Delta b_k$ for a collision, labeled j ($1\leqslant j\leqslant N$). The weights (w_k) were taken according to Simpson's rule and the range of integration covered all values of the impact parameter for which $p^{c,i}(j,b_j)\neq0$. The accumulation of errors in the numerical integration of the equations of motion was monitored by

TABLE I. Total antiproton capture cross sections, $\sigma^c=\Sigma_{nl}\sigma^c_{nl}$, for an atomic hydrogen target, as a function of the center-of-mass collision energy, E.

E (a.u.)	σ^c (πa_0^2)	E (a.u.)	σ^c (πa_0^2)
0.100	5.03	0.430	2.73
0.125	4.44	0.460	2.68
0.150	4.10	0.480	2.62
0.175	3.83	0.500	2.58
0.200	3.62	0.510	2.49
0.225	3.48	0.520	2.20
0.250	3.36	0.530	1.85
0.275	3.25	0.540	1.40
0.300	3.14	0.550	1.02
0.325	3.03	0.560	0.64
0.350	2.96	0.580	0.31
0.375	2.88	0.600	0.16
0.400	2.81	0.620	0.09

TABLE II. Total pion capture cross sections ($\sigma^c=\Sigma_{nl}\sigma^c_{nl}$) for π^- collisions with an atomic hydrogen target, as a function of the center-of-mass collision energy, E.

E (a.u.)	σ^c (πa_0^2)	E (a.u.)	σ^c (πa_0^2)
0.100	5.13	0.500	2.65
0.120	4.67	0.520	2.42
0.150	4.20	0.540	2.08
0.200	3.73	0.560	1.64
0.250	3.47	0.580	1.16
0.300	3.22	0.600	0.76
0.350	3.03	0.620	0.44
0.400	2.90	0.640	0.31
0.425	2.82	0.660	0.19
0.450	2.74	0.680	0.14
0.480	2.71	0.700	0.11

regular checks of the conservation laws. For example, in laser-free collisions, when energy conservation is violated by one part in 10 000, the results were discarded from the sample. A small number of orbits failed to converge to a prescribed exit channel as $t\to\infty$, and these were also rejected. In all, it was found that these anomalous results never exceeded 0.1% of the total number of collisions and thus much less than statistical fluctuations in the sampling process.

III. FIELD-FREE ANTIPROTON CAPTURE

Results for antiproton capture and collisional ionization were used to establish the accuracy of our code and to extend the range of the data. The statistical errors, denoted by the standard deviation s, are very much smaller than the point sizes on the figures. Sample results for the hydrogen target are given in Table I and agree well with previous simulations [11]. We also present results for π^- ($m_\pi\approx 273m_e$) capture by hydrogen in Table II. It has been noted [7] that cross sections for capture of μ^- ($m_\mu\approx 207m_e$) [7,13,14,16] and $\bar{p}$ by hydrogen are very similar, and our data for π^- follow this trend. This reflects the fact that the electron ejection process at low energies involves a centrifugal energy barrier against the incident particle approaching the critical distance of ionization, rather than a condition dependent on the collision velocity [6]. Our data are more extensive and statistically accurate than previous CTMC simulations [11,14,7,17]. As an example of the sampling error, the cross section for capture for $E=0.2$, given by $\sigma^c=3.62\pi a_0^2$, was obtained from $N=5\times 10^4$ trajectories, which equates to a standard deviation of $s=0.02\pi a_0^2$. Similarly, the cross section for collisional ionization (σ^i) of positronium for $E_{\rm lab}=10$ keV given by $\sigma^i=0.32\pi a_0^2$ was obtained from $N=10^5$ trajectories with $s=0.01\pi a_0^2$.

The distribution of antiprotons in subshells (σ^c_{nl}) has been considered by Cohen [7,18]. If the electron is liberated with an energy $\varepsilon>0$ (in the center-of-mass frame), then the protonium energy $E_n=-\mu_{23}/(2n^2)$ is determined by $E_n=E-\frac{1}{2}\mu_{12}-\varepsilon$. Slow electron escape, $\varepsilon\approx 0$, means that capture must occur near the level $n_{\rm max}\approx\sqrt{\mu_{23}/(\mu_{12}-2E)}$. This corresponds closely to our data (Fig. 1); for example, at $E=0.05$ the formula gives $n_{\rm max}\approx 32$. The sharpness of the σ^c_n distributions indicates a thin capture shell around the atom corresponding to $n\gg 1$ and partially explains why classical theory works rather well in this instance. At higher energies, the ejected electron energy spectrum is broader, corresponding to antiproton-electron collisions in which momentum and energy transfer is required to effect capture. This leads to a broadening in the σ^c_n distribution, and the maximum of the curve favors lower n. The target atom has spherical symmetry, and thus the summation over all n and m levels yields cross sections that reflect the statistical weight: $\sigma^c_l\propto(2l+1)$ [6]. In Fig. 2, the distributions, σ^c_l, follow this trend until the cutoff at $l\sim n_{\rm max}$ corresponding to the n distribution (Fig. 1). Using the semiclassical correspondence $l\sim\mu_{12,3}vb$,

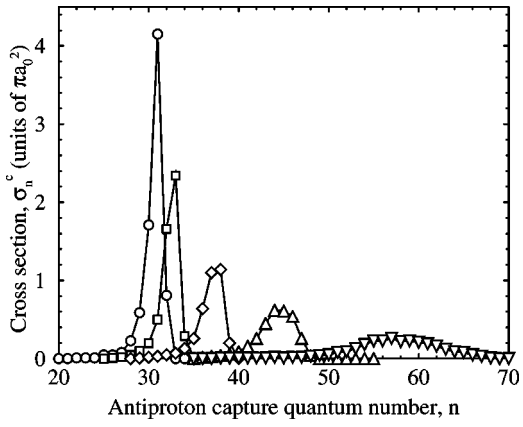

FIG. 1. Partial cross sections, $\sigma^c_n=\Sigma_l\sigma^c_{nl}$, for protonium formation in a quasiquantum level n, following antiproton-hydrogen collisions. Center-of-mass collision energy in atomic units: ○, $E=0.05$; □, $E=0.1$; ◇, $E=0.2$; △, $E=0.3$; ▽, $E=0.4$.

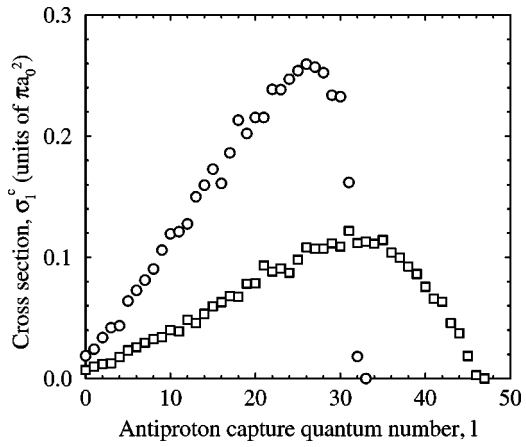

FIG. 2. Partial cross sections $\sigma_l^c = \Sigma_n \sigma_{nl}^c$ for protonium formation in a quasiquantal state l following antiproton-hydrogen collisions. Center-of-mass collision energy in atomic units: ○, $E=0.1$ and □, $E=0.3$.

Fig. 2 can also be viewed as the weighted capture probability $bp^c(b)$, which is sharply attenuated for orbits that pass outside the capture radius (R_c). The antiprotons that are captured occupy a wide distribution of states. A small fraction of these capture antiprotons moves in nearly circular orbits $l \sim n$. These orbits are associated with long-lived states of antiprotonic helium [3]. At energies above the ionization threshold, the capture cross section falls away rapidly as a result of the requirement for momentum matching [19].

Antiproton collision with positronium has been proposed as an efficient means of producing cold antihydrogen [1]. Our CTMC results are shown in Fig. 3 along with previous results for $E_{\rm lab} > 2$ keV by Ermolaev [17]. The results agree very well with experimental results [20] for the charge-conjugate reaction $p + \mathrm{Ps} \rightarrow \mathrm{H} + e^+$. In [20], the cross section for hydrogen formation at 13.3 keV is determined to be $\sigma^c = 9 \pm 3 \pi a_0^2$ compared with our results of $10 \pi a_0^2$; and at $E_{\rm lab} = 11.3$ keV, $\sigma^c = 30 \pm 10 \pi a_0^2$, compared with the CTMC results: $15 \pi a_0^2$.

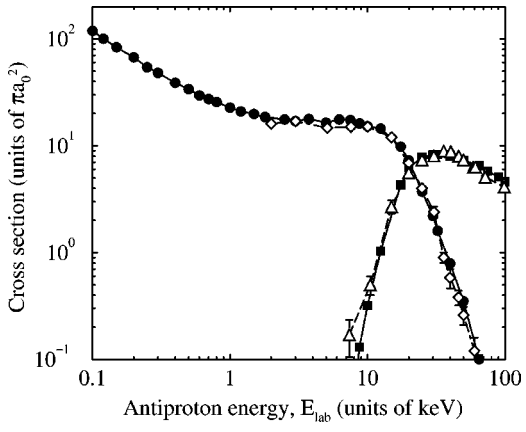

FIG. 3. Capture ● and ionization ■ cross sections for antiproton impact on positronium, and their dependence on the antiproton kinetic energy, $E_{\rm lab}$. Comparison with CTMC results of Ermolaev [17] for capture ◇ and ionization △. The laboratory ($E_{\rm lab}$) and center-of-mass energy (E) are related by Eq. (2.3).

TABLE III. Capture (σ^c) and ionization (σ^i) cross sections for antiproton ($\bar{p}$) collisions with positronium (Ps) as a function of the laboratory collision energy $E_{\rm lab}$. The laboratory ($E_{\rm lab}$) and center-of-mass energy (E) are related by Eq. (2.3).

$E_{\rm lab}$ (keV)	σ^c (πa_0^2)	$E_{\rm lab}$ (keV)	σ^c (πa_0^2)	σ^i (πa_0^2)
0.10	119.0	5.00	16.4	0.00
0.12	100.0	6.25	17.6	0.00
0.15	83.7	7.50	17.4	0.02
0.20	67.2	8.75	16.2	0.13
0.25	54.4	10.0	15.2	0.32
0.30	48.0	12.5	14.5	1.0
0.40	38.9	17.5	9.8	4.3
0.50	33.9	20.0	7.3	6.2
0.60	29.5	25.0	3.7	7.8
0.70	27.4	30.0	2.2	8.2
0.80	25.6	32.5	1.6	8.3
1.00	23.0	40.0	0.79	8.0
1.20	21.0	50.0	0.35	7.3
1.50	19.8	65.0	0.10	6.5
1.80	18.6	75.5	0.05	5.8
2.50	17.6	90.0	0.00	5.1
3.00	17.0	100	0.00	4.6
3.75	17.8			

It can be seen in Fig. 3 that the capture cross section for positronium has a prominent plateau feature over the energy range 2–10 keV. This is suggestive of a geometric target corresponding to a critical capture radius. Employing the laws of conservation of energy and angular momentum, and assuming that capture occurs at an antiproton-positron radius (R_c) where the electronic energy becomes positive, we arrive at the formula [14] for the cross section in terms of the critical distance:

$$\sigma^c = \kappa \pi R_c^2 [1 + E^{-1}(R_c^{-1} + \varepsilon_i)], \tag{3.1}$$

where $\kappa \leqslant 1$ is an empirical factor introduced to represent the efficiency of capture and $\varepsilon_i = -\frac{1}{2}\mu_{12}$ is the target energy. If we assume that R_c corresponds to the limit of the classical electron distribution, this simple model seems to explain the general trends in Tables I, II, and III. In fact, the data are very well represented by the following fits for the parameters: for $\bar{p}+\mathrm{Ps}$, $R_c = 3.5$ and $\kappa = 0.96$; for $\bar{p}+\mathrm{H}$, the fit is not quite as good, and we find that $R_c = 1.60, \kappa = 0.87$ gives a reasonable approximation to the data. Given that the Ps radius is twice as large as that of H, one might expect that $R_c(\bar{p}+\mathrm{Ps}) \approx 2R_c(\bar{p}+\mathrm{H})$. We find from the fitted values that this is true to a good approximation. The capture radius model suggests that an increase in the antihydrogen production cross section might be obtained if the positronium could be either excited or polarized by an external field. In simple terms, the atom would have a larger orbit and charge volume and hence R_c would be increased.

IV. LASER-ASSISTED ANTIHYDROGEN FORMATION

The enhancement of capture due to laser assistance has been studied in the Born approximation [21]. However, it has been confirmed [6] that for laser-free collisions this model is inadequate at energies below the ionization threshold [19] in that it grossly overestimates the capture process. Nonetheless, calculations at high energies using this approximation predicted an enhancement of capture in some circumstances by a factor of 10 or more [21,23] when an intense laser was present. However, a closer analysis revealed that, at the laser intensities considered, rapid photoionization [22] would dominate the process and thus prevent capture from occurring. We consider the process over the energy range of interest to experiment. In particular, we investigate laser-assisted formation of antihydrogen at two collision energies, $E_{\rm lab}=1$ keV and 15 keV for $\lambda=248$ nm and $\lambda=1064$ nm, and we consider linear polarized light with alignment parallel and perpendicular to the collision axis (direction of the antiproton beam).

Classical models of photoionization have been used successfully in the qualitative understanding of the response of atoms to intense light [24]. In order to test our classical model of laser-positronium interaction quantitatively, we calculated the photoionization rate of isolated positronium. We considered two field strengths, $F_{\rm max}=0.01$ a.u. and 0.02 a.u., corresponding to intensities of $I=3.5\times10^{12}$ W cm^{-2} and $I=1.4\times10^{13}$ W cm^{-2}, respectively. The ionization yield was calculated for a variety of pulse lengths to establish a photoionization rate Γ. At $I=3.5\times10^{12}$ W cm^{-2}, the classical model predicts that very little ionization will occur, $\Gamma_c<2\times10^{-7}$. For the stronger field ($F=0.02$), the results are $\Gamma_c=1.2\times10^{-4}$ for $\lambda=248$ nm and $\Gamma_c=1.1\times10^{-4}$ for $\lambda=1064$ nm. These results were compared to accurate quantal calculations [25], which, for $\lambda=248$ nm, predict $\Gamma_q=1.80\times10^{-4}$ for $F_{\rm max}=0.01$ and $\Gamma_q=1.26\times10^{-3}$ for $F_{\rm max}=0.02$. For $\lambda=1064$ nm, the quantal rates are estimated at $\Gamma_q\approx1.5\times10^{-5}$ for $F_{\rm max}=0.01$ and $\Gamma_q=4\times10^{-3}$ for $F_{\rm max}=0.02$. These results confirm that classical models can underestimate multiphoton ionization rates by large factors. Note that for long-wavelength high-intensity light, the dominant mechanism of photoionization is through tunneling (field-ionization) transitions, a process that is classically forbidden.

For $E_{\rm lab}=1$ keV, with an initial internuclear separation of $d=40$, the laser was ramped on over a time $\tau\approx80$. The results we obtained did not show any variation under changes in the pulse rise time over the range $40<\tau<120$. Given the optical cycle times are 147 a.u. for $\lambda=1064$ nm and 34 a.u. for $\lambda=248$ nm, the random laser phase φ must be taken into account by statistical averaging. Displayed in Table IV are results for laser-assisted antihydrogen formation. At $E_{\rm lab}=1$ keV, an increase of 4–70 % in the capture cross section was observed. The direction of the laser polarization vector, and hence the orientation of the positronium orbit, was not an important factor, and supports the critical distance model of capture.

At the higher energy, $E_{\rm lab}=15$ keV, the capture process is thought to be a sudden transition, for which the momentum and position distribution of the target is more significant. The enhancement created by parallel polarization can be understood in terms of the laser driving the electron along the beam axis and creating more favorable conditions for momentum exchange between the projectile and ejectile. Our estimates of ionization events show that collisional ionization was greatly enhanced. Indeed, the combination of laser and antiproton was effective in producing ionization of the positronium in circumstances in which neither were effective alone. For some cases, the ionization yields increased at the expense of the capture cross section. Significant enhancement of capture requires a strong laser field. However, destruction of the positronium target by photoionization becomes a practical problem in implementation of this scheme. In order to inhibit this process, the laser interaction might be separated from the collision process by using pulsed light or passing positronium through the laser focus. Consider a configuration in which a positronium beam crosses the diffraction-limited spot of a light source of $\lambda=248$ nm. An energy of the order $E_{\rm lab}\sim1$ keV would equate to a relative speed of $v\sim0.2$ a.u. Thus the positronium-laser interaction time would be of the order 10^4 atomic units. Clearly, photoionization rates in excess of $\Gamma\sim1\times10^{-4}$ would mean significant loss of positronium. Thus the scheme would require a careful choice of laser wavelength and intensity.

TABLE IV. Antiproton capture cross sections (σ_L^c) for antiproton impact on positronium in the presence of a laser field. Laser polarization is linear and either parallel ($\parallel$) or perpendicular ($\perp$) to the antiproton beam. The laboratory and center-of-mass energies are related by Eq. (2.3).

$E_{\rm lab}$ (keV)	Field strength $F_{\rm max}$ (a.u.)	λ (nm)	Laser polarization	σ_L^c (πa_0^2)
1	. . . . .	without laser	. . . . .	23.0
	0.01	1064	$\perp$	24.3
			$\parallel$	25.5
		248	$\perp$	24.0
			$\parallel$	24.0
	0.02	1064	$\perp$	25.2
			$\parallel$	27.8
		248	$\perp$	39.0
			$\parallel$	40.0
15	. . . . .	without laser	. . . . .	12.1
	0.01	1064	$\perp$	9.8
			$\parallel$	11.0
		248	$\perp$	12.0
			$\parallel$	13.1
	0.02	1064	$\perp$	7.0
			$\parallel$	10.4
		248	$\perp$	11.0
			$\parallel$	13.0

V. CONCLUSIONS

In this paper, we simulated the classical capture of slow antiprotons by atomic hydrogen and positronium. The effect

of a laser field on antiproton capture by positronium was investigated. Within the limitations of the classical model, statistically accurate cross sections for protonium and antihydrogen formation were obtained and the energy dependence of the process was established. The results agree very well with experimental data for proton capture by positronium [20]. The present calculations found that the addition of the laser field led to enhancement of the formation of antihydrogen of 4–70 % for a collision energy of 1 keV. Our conclusion is that, in the synthesis of antihydrogen, the addition of a laser field would act as a useful accelerant. While the classical model has shortcomings, these preliminary results are promising. A more authoritative statement on the viability of such schemes would require quantal modeling of low-energy laser-assisted antiproton capture by positronium, or equivalently laser-assisted positron-atom scattering leading to the formation of positronium. Such a study seems warranted and worthwhile.

ACKNOWLEDGMENTS

This work was supported by the Engineering and Physical Sciences Research Council (EPSRC), the British Council, and the Japan International Science and Technology Exchange Center (JISTEC). One of us (R.J.W.) would also like to thank the staff at RIKEN, Japan for their hospitality during a visit in which some of this work was undertaken. We are most grateful to Dr. Y. Teranishi (RIKEN) for his contribution to our discussions. We would also like to thank Robert Potvliege for supplying us with Floquet results for photoionization of positronium and for very helpful communications with Dr. K. Ohtsuki.

[1] M. Charlton, J. Eades, D. Horváth, R. J. Hughes, and C. Zimmermann, Phys. Rep. **241**, 65 (1994).
[2] M. Iwasaki *et al.*, Phys. Rev. Lett. **67**, 1246 (1991).
[3] T. Yamazaki *et al.*, Phys. Rev. A **55**, R3295 (1997).
[4] H. A. Torii *et al.*, Phys. Rev. A **59**, 223 (1999), and references cited therein.
[5] H. Knudsen and J. F. Reading, Phys. Rep. **212**, 107 (1992).
[6] J. S. Cohen, in *The Physics of Electronic and Atomic Collisions*, edited by Y. Itikawa *et al.* (AIP, Melville, NY, 2000), p. 540.
[7] J. S. Cohen, Phys. Rev. A **36**, 2024 (1987).
[8] R. Abrines and I. C. Percival, Proc. Phys. Soc. **88**, 861 (1966).
[9] R. E. Olson, Phys. Rev. A **24**, 1726 (1981).
[10] C. L. Kirschbaum and L. Wilets, Phys. Rev. A **21**, 834 (1980).
[11] J. S. Cohen, Phys. Rev. A **56**, 3583 (1997).
[12] J. S. Cohen, J. Phys. B **31**, L833 (1998).
[13] N. H. Kwong, J. D. Garcia, and J. S. Cohen, J. Phys. B **22**, L633 (1989).
[14] J. S. Cohen, Phys. Rev. A **27**, 167 (1983).
[15] Numerical Algorithms Library (NAg), subroutine D02PDF.
[16] J. S. Cohen, R. L. Martin, and W. R. Wadt, Phys. Rev. A **24**, 33 (1981).
[17] A. M. Ermolaev, Hyperfine Interact. **44**, 375 (1988).
[18] J. S. Cohen and N. T. Padial, Phys. Rev. A **41**, 3460 (1990).
[19] B. H. Bransden, C. J. Joachain, and J. F. McCann, J. Phys. B **25**, 4965 (1992).
[20] J. P. Merrison *et al.*, Phys. Rev. Lett. **78**, 2728 (1997); Hyperfine Interact. **109**, 313 (1997).
[21] S.-M. Li *et al.*, Phys. Rev. A **59**, 1697 (1999).
[22] L. B. Madsen and P. Lambropoulos, Phys. Rev. A **61**, 067401 (2000).
[23] S.-M. Li *et al.*, Phys. Rev. A **61**, 067402 (2000).
[24] G. Bandarage, A. Maquet, and J. Cooper, Phys. Rev. A **41**, 1744 (1990).
[25] R. M. Potvliege, Comput. Phys. Commun. **114**, 42 (1998).